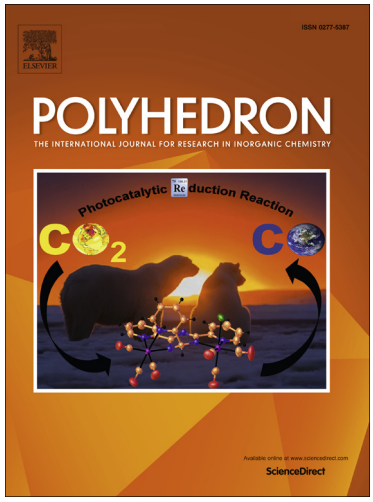

Synthesis, characterization and biological activity of platinum (II) complexes with a tetrapyrazole ligand

Angel R. Higuera-Padilla, Jorlis Capote, Dianela Ortega, William Castro, Mildred Rodriguez-Cordero, David Coll, Fernando Hernández-Medina, Mercedes Fernández-Mestre, Izaskun Urdanibia, Peter Taylor, Barbara Rodriguez, Arquímedes Karam

PII: S0277-5387(15)00575-6
DOI: http://dx.doi.org/10.1016/j.poly.2015.09.065
Reference: POLY 11579

To appear in: *Polyhedron*

Received Date: 26 May 2015
Accepted Date: 30 September 2015

Please cite this article as: A.R. Higuera-Padilla, J. Capote, D. Ortega, W. Castro, M. Rodriguez-Cordero, D. Coll, F. Hernández-Medina, M. Fernández-Mestre, I. Urdanibia, P. Taylor, B. Rodriguez, A. Karam, Synthesis, characterization and biological activity of platinum (II) complexes with a tetrapyrazole ligand, *Polyhedron* (2015), doi: http://dx.doi.org/10.1016/j.poly.2015.09.065

Synthesis, characterization and biological activity of platinum (II) complexes with a tetrapyrazole ligand

Angel R. Higuera-Padilla[a,*], Jorlis Capote[a,b], Dianela Ortega[a], William Castro[a], Mildred Rodriguez-Cordero[c], David Coll[d], Fernando Hernández-Medina[e], Mercedes Fernández-Mestre[e], Izaskun Urdanibia[f], Peter Taylor[f], Barbara Rodriguez[g], Arquímedes Karam[h,*]

[a] Laboratorio de Química Bioinorgánica, Centro de Química, Instituto Venezolano de Investigaciones Científicas (IVIC), Caracas 1020-A, Venezuela

[b] Universidad Central de Venezuela, Caracas, Venezuela

[c] Laboratorio de Química Bioinorgánica. Universidad Simón Bolívar, Caracas, 1080, Venezuela

[d] Laboratorio de Química Computacional, Centro de Química, Instituto Venezolano de Investigaciones Científicas (IVIC), Caracas 1020-A, Venezuela

[e] Laboratorio de Fisiopatología sección Inmunogenética, Centro de Medicina Experimental, Instituto Venezolano de Investigaciones Científicas (IVIC), Caracas 1020-A, Venezuela

[f] Laboratorio de Patología Celular y Molecular, Centro de Medicina Experimental, Instituto Venezolano de Investigaciones Científicas (IVIC), Caracas 1020-A, Venezuela

[g] Departamento de Química Inorgánica, Facultad de Química, Pontificia Universidad Católica de Chile, Casilla 306, Santiago-609441, Chile.

[h] Laboratorio de Polímeros, Centro de Química, Instituto Venezolano de Investigaciones Científicas (IVIC), Caracas 1020-A, Venezuela

[*] Corresponding authors. Tel.: +58 212 5041775/1832. E-mail addresses: angelruben@hotmail.com (A.R. Higuera-Padilla), akaram@ivic.gob.ve (A. Karam)

In the search of an effective chemotherapy for the treatment of cancer, in this work we describe the synthesis, characterization and biological activity of two new platinum complexes. The general formula is $[Pt_2(L)(X)_4]$, where **L** was 1,2,4,5-tetrakis((1*H*-pyrazol-1-yl)methyl)benzene and X were iodine (**1**) and chlorine (**2**). The most probable structure was established through a combination of spectroscopic analysis and density functional theory (DFT) calculations. Studies of interaction of complexes with DNA were carried out, and the results by spectroscopic titrations, thermal denaturation and viscosity, showed noncovalent interactions of complexes with DNA. The comet assay showed damage to cellular DNA. Inhibition assays of thioredoxin reductase (TrxR) were carried out, and the compounds showed notable inhibitory activity on the enzyme in a concentration dependent manner, with IC_{50} values of 3.9 and 3.5 nM for **1** and **2** respectively. Complex **2** exhibited greater inhibitory effects than complex **1** against all the tumor cell lines, with growth inhibitory effects superior to cisplatin in some cases.

Keywords: Anticancer activity, platinum complexes, DNA, Thioredoxin reductase.

Introduction

According to the World Health Organization, cancer figures among the leading causes of death worldwide, accounting for 8.2 million deaths in 2012 [1]. In the search of an effective

chemotherapy for the treatment of cancer, the coordination of organic molecules to metal centers is a strategy that has attracted the attention of the scientific community for its remarkable outcomes [2].

The use of platinum compounds as anticancer agents originated in the 1960´s, with the serendipitous discovery of cisplatin [3], the first platinum drug used against cancer, which is still widely used today [4]. Since the discovery of the activity of cisplatin against this disease, bioinorganic and medicinal chemists have been looking for new platinum-containing agents [5,6,7]. It has been broadly demonstrated that platinum compounds exert their effect through interaction with DNA [8,9], bonding covalently. Moreover, pyrazole-derived compounds are used for their biological properties [10], as analgesic [11], antiglycemic [12], antiallergic [13], anti-inflammatory [14], antibacterial [15], antiparasitic [16], antiviral [17] and anticancer agents [18,19]. Thus it is clear that the pyrazole moiety holds promise in medicine; in fact, complexes with nitrogen-donor ligands in general have shown good biological activities for different ailments [20].

Taking in account that metals impart activity to ligands [20], the strategy in this study was to combine the activity of the pyrazole moiety with the metal center to achieve a synergic effect in the biological response [21,22]. We present here the synthesis and characterization of two new platinum–tetrapyrazole complexes, their interaction with DNA, TrxR inhibition assays and cytotoxic activity against six different cancer cell lines.

Materials and methods

Chemicals

All manipulations were routinely carried out under N_2 using common Schlenck techniques. Solvents were purified using standard procedures immediately prior to use. Starting material 1,2,4,5-tetrakis(bromomethyl)benzene, pyrazole and potassium iodide were obtained from Sigma-Aldrich. K_2PtCl_4 was acquired from Strem Chemicals. The pyrazole derivative **L** was synthesized with slight modifications to a reference previously published [23]. Melting points were measured on a Buchi apparatus. C, H and N analyses were performed with a Carlo Erba EA1108 elemental analyzer. NMR spectra were obtained in $CDCl_3$ and in a DMSO-d_6 solution in a Bruker AVANCE 300 spectrometer. ^{1}H NMR shifts were recorded relative to residual proton resonances in the deuterated solvent. IR spectra were obtained with a Nicolet Magna IR 560 spectrometer. UV–vis spectra were recorded on a HP 8453 diode array instrument. ESI mass

spectra were obtained by using a Thermofinnigan LXQ spectrometer with chloroform as the solvent.

[1,2,4,5-tetrakis((1*H*-pyrazol-1-yl)methyl)benzene] (L)

Ligand 1,2,4,5-tetrakis((1*H*-pyrazol-1-yl)methyl)benzene was synthesized with slight modification to a previously reported method [23]. A mixture of 1,2,4,5-tetrakis(bromomethyl)benzene (544.5 mg, 1.21 mmol), pyrazol (362.8 mg, 5.33 mmol), sodium hydroxide 40% (NaOH, 2.5 mL) and tetrabutylammonium hydroxide 40% (TBAH, 1 mL), was refluxed in toluene (14 mL) for 24 hours. This dark brown solution was filtered off after addition of 20 mL of water. The pale yellow solid was washed with water and diethyl ether then dried under vacuum. Yield: 70%. Melting point: 173-175 ºC. Elemental analysis (%) Calc. for $(C_{22}H_{22}N_8) \cdot H_2O$: C 63.45; N 26.90; H 5.81. Found: C 63.28; N 26.67; H 5.43. ESI-MS ($CHCl_3$): (L+) m/z 399.28. IR (KBr, cm^{-1}): ν(C=C) 1633, ν(C=N) 1514, ν(C–H) 3121. ^{1}H NMR (DMSO-d_6) (ppm) 7.65 (d, 4H, J(Hz) = 2.01); 7.42 (d, 4H, J(Hz) = 1.45); 6.63 (s, 2H); 6.23 (t, 4H); 5.38 (s, 8H). ^{13}C NMR (DMSO-d_6) (ppm) 139.04 (C3´); 135.30 (C1, C2, C4, C5); 130.14 (C5´); 129.05 (C3, C6); 105.56 (C4´); 51.50 (C7). UV-vis (DMSO) 268 nm. $\varepsilon_{(268\ nm,\ DMSO)}$ = 437 $M^{-1}cm^{-1}$.

[Pt_2LI_4] (1)

Potassium iodide – KI (392.4 mg; 2.37 mmol) was added to a solution of K_2PtCl_4 (50.7 mg; 0.12 mmol) in water (10 mL) followed by a solution of **L** (47.9 mg; 0.12 mmol) in ethanol (4 mL) and the mixture was stirred. A yellow solid precipitated immediately. This was filtered off and washed with water and diethyl ether, then dried under vacuum. Yield: 65%. Melting point: 290-292 ºC. Elemental analysis (%) Calc. for ($C_{22}H_{22}I_4N_8Pt_2$): C 20.38; N 8.64; H 1.71. Found: C 20.86; N 8.98; H 1.88. ESI-MS ($CHCl_3$): (M – I) m/z 1168.84. IR (KBr, cm^{-1}): ν(C=C) 1624, ν(C=N) 1518, ν(C–H) 3108. ^{1}H NMR (DMSO-d_6) (ppm) 7.64 (d, 4H, J(Hz) = 2.01); 7.42 (d, 4H, J(Hz) = 1.45); 6.62 (s, 2H); 6.23 (t, 4H); 5.37 (s, 8H). ^{13}C NMR (DMSO-d_6) (ppm) 139.02 (C3´); 135.20 (C1, C2, C4, C5); 130.14 (C5´); 128.95 (C3, C6); 105.50 (C4´); 51.44 (C7). UV-vis (DMSO) 262 nm. $\varepsilon_{(262\ nm,\ DMSO)}$ = 13229 $M^{-1}cm^{-1}$.

[Pt_2LCl_4] (2)

K_2PtCl_4 (104.5 mg, 0.25 mmol) was dissolved in distilled water and a solution of **L** (50.5 mg, 0.13 mmol) in ethanol was added. The mixture was stirred at room temperature for 36 h. The yellow precipitate was filtered off, washed with water and diethyl ether, and then dried under

vacuum. Yield: 72%. Melting point: > 350 ºC. Elemental analysis (%) Calc. for ($C_{22}H_{22}Cl_4N_8Pt_2$): C 28.40; N 12.04; H 2.38. Found: C 29.10; N 11.81; H 2.82. ESI-MS ($CHCl_3$): (M – Cl) m/z 895.09. IR (KBr, cm^{-1}): ν(C=C) 1623, ν(C=N) 1518, ν(C–H) 3106. ^{1}H NMR (DMSO-d_6) (ppm) 7.54 (d, 4H, J(Hz) = 2.25); 7.38 (d, 4H, J(Hz) = 1.83); 6.71 (s, 2H); 6.19 (t, 4H); 5.34 (s, 8H). ^{13}C NMR (DMSO-d_6) (ppm) 138.97 (C3´); 135.24 (C1, C2, C4, C5); 130.06 (C5´); 129.04 (C3, C6); 105.50 (C4´); 51.46 (C7). UV-vis (DMSO) 260 nm. $\varepsilon_{(260\ nm,\ DMSO)}$ = 5426 $M^{-1}cm^{-1}$.

Computational methods

All structures were optimized using DMol [3] [24,25,26]. This DFT-based program permits determination of the relative stability of all studied species based on their electronic structure. The calculations were performed using the Kohn-Sham Hamiltonian method with the Perdew-Wang 1991 gradient correction [27] and the double-zeta plus (DNP) numerical basic set, which provides good accuracy at a relatively low computational cost. The All Electron core treatment was used for all the atoms. Frequency calculations of the structures showed that all frequencies were positive indicating that all structures are real minima.

DNA studies

All the measurements with calf thymus (ct) DNA were carried out in Tris–HCl 5 mM buffer (pH 7.2), 50 mM NaCl. The UV absorbance ratio $\lambda_{260}/\lambda_{280}$ was 1.81 indicating that the DNA was essentially free of protein [28]. The ctDNA concentration per nucleotide was determined by absorption spectrophotometric analysis using the molar absorption coefficient 6600 $mol^{-1}dm^3cm^{-1}$ at 260 nm [29].

The spectroscopic titrations were carried out by adding increasing amounts of ctDNA to a solution of the complex at a fixed concentration in a quartz cell, and recording the UV–Vis spectra after each addition [30]. The absorption by DNA was subtracted by adding the same amounts of ctDNA to the blank. The intrinsic binding constant K_b was determined from the plot of [DNA]/(e_a - e_f) vs [DNA], where [DNA] is the concentration of DNA in base pairs, and the apparent absorption coefficients, ε_a, ε_f, ε_b correspond to A_{obs}/[Pt], the extinction coefficient for the free platinum complex and the extinction coefficient of the platinum complex in the totally bound form, respectively [31]. The data were fitted to Eq. 1, with a slope equal to 1/(ε_b - ε_f) and

the intercept equal to $1/[Kb(\varepsilon_b - \varepsilon_f)]$. Kb was obtained from the ratio of the slope to the intercept [32].

$$[DNA] / (\varepsilon_a - \varepsilon_f) = [DNA] / (\varepsilon_b - \varepsilon_f) + 1 / [K_b (\varepsilon_b - \varepsilon_f)] \quad \text{(Eq. 1)}$$

Viscosity measurements were carried out using an Ostwald viscometer immersed in a water bath maintained at 25 °C. The DNA concentration was kept constant in all samples, while the complex concentration was increased from 0 to 67 μM. The flow time was measured at least 6 times with a digital stopwatch and the mean value was calculated. Data are presented as $(\eta/\eta^0)^{1/3}$ versus the ratio [complex]/[DNA], where η and η^0 are the specific viscosity of DNA in the presence and absence of the complex, respectively. The values of η and η^0 were calculated from the expression $(t - t^b)/t^b$, where t is the observed flow time and t^b is the flow time with buffer alone. The relative viscosity of the DNA was calculated from η/η^0 [33].
The interactions of the complexes with ctDNA were also measured in thermal denaturation experiments. Melting curves were recorded in media containing 50 mM $NaClO_4$ and 5 mM Tris/HCl buffer (pH = 7.29). The absorbance of the ctDNA solution (~ 60 μM) was monitored at 260 nm before and after incubation with the drug (~ 7 μM in Tris/HCl buffer) for 1 h at room temperature. The temperature was increased by 1 ºC/min between 65 and 85 ºC and by 3ºC/min between 40 and 65 ºC and between 85 and 94 ºC [34,35].

Comet assay

Heparinized whole blood was collected by venipuncture from donor and lymphocytes separated using Hypaque 1047 (Sigma-Aldrich, St. Louis, USA). The cells were washed twice with PBS supplemented with EDTA and FBS, and resuspended in RPMI-1640 medium supplemented with FBS and L-glutamine. Treatments were 24 h in the same supplemented medium. To an eppendorf tube was added 1 mL of supplemented medium containing and appropriates volumes of compounds. Cells were incubated in the presence of the compounds (5 – 30 μM) at $5x10^5$ cells /well for 24 h in 12-well plates at 37°C, then resuspended in 250 μL of low melting point agarose gel (LMA) for embedding on slides. Cells were checked for viability by trypan blue exclusion (viability > 95%). The technique followed for the slide preparation was previously described by Tice and Strauss[36]. The slides were each covered with 110 μL of 0.5% normal melting agarose (NMA) at about 50°C in Ca^{2+} and Mg^{2+} free PBS and then kept at room temperature for about 5 minutes to allow the agarose to solidify. This layer was used to promote

the attachment of the second layer. Around 10,000 cells were mixed and rapidly pipetted onto the first agarose layer, and spread using a coverslip, and maintained on an ice-cold flat tray for 5 minutes to solidify. After removal of the coverslip, the slides were immersed in freshly prepared cold lysing solution (2.5 M NaCl, 100 mM Na_2EDTA, 10 mM Tris, pH 10) with 1% Triton X-100 and 10% DMSO overnight at 4°C in a covered dish. The slides were then drained and placed in a gel electrophoresis tank. The slides were left in electrophoresis solution under alkaline conditions (1 mM Na_2EDTA and 300 mM NaOH, pH 13) for 30 min to allow the unwinding of the DNA and expression of alkali labile damage before electrophoresis. Electrophoresis was conducted with cold electrophoresis solution for 30 minutes at 25 V and 300 mA. All of these steps were conducted under dimmed light to prevent the occurrence of additional DNA damage. After electrophoresis, the slides were immersed in neutralization buffer (0.4 M Tris, pH 7.5) for 5 min to eliminate the excess alkali then allowed to air dry. Finally, 160 µL of ethidium bromide (10 mg/mL) were added to 200 mL of distilled water and slides were immersed in the staining solution for 1-3 min. The slides were analyzed with an Array Scan VTI imaging system (Thermo Scientific).

Interaction with thioredoxin reductase

TrxR inhibition experiments were carried out using a TrxR rat liver kit and bovine serum albumin (BSA), both obtained from Sigma-Aldrich. Enzyme was diluted to 0.5 µg/mL in phosphate buffer (pH 7.0, with 20 mM EDTA, 20 µg/mL BSA) and incubated for 10 min in flat-bottom wells at room temperature with different concentrations of complex dissolved in DMSO. In the case of the control sample, an equivalent volume of DMSO was added to the working buffer. After this time, the reaction was initiated with the addition of 5,5´-dithiobis (2-nitrobenzoic acid) (DTNB, included in the kit), which is reduced by the enzyme system providing a direct measurement of the TrxR activity [37]. The kinetics was studied for about 16 minutes, taking measurements every 16 seconds in a TECAN Sunrise absorbance reader.

Growth inhibition and cytotoxicity

Five human and one murine tumor cell lines were used. MCF-7 (human breast carcinoma), PC-3 (human prostate carcinoma), A459 (human lung carcinoma), HeLa (human cervical carcinoma), HT-29 (human colon carcinoma), and 4T1 (murine breast carcinoma) cells were cultured in Dulbecco's Modified Eagle's Medium (DMEM) supplemented with 10% heat-inactivated fetal

bovine, (Gibco, BRL, USA) and penicillin (100 Units/mL) / streptomycin (100 μg/mL), containing, in addition, glucose 0.45% for the HT-29 cells. The sulphorhodamine B (SRB) assay was used to evaluate the effect of the compounds on the growth and viability of the six tumor cell lines [38]. Each drug was assayed in triplicate at 7 different concentrations up to a maximum of 30 μM. The concentrations inducing 50% growth inhibition (GI_{50}), total growth inhibition (TGI) and 50% cytotoxicity (LC_{50}) after a 48 h incubation period were calculated by linear interpolation from the observed data points.

Results and discussion

Synthesis and characterization

L was synthesized following a previously reported method with slight modifications [23]. This was achieved through the condensation of 1,2,4,5-tetrakis(bromomethyl)benzene with pyrazole (commercially availables) in the presence of 40% NaOH and 40% tetrabutylammonium hydroxide solution (TBAH) in refluxing toluene with 70% yield (improved with this methodology), after purification by recrystallization (Figure 1). The pale yellow solid was washed with water and diethyl ether then dried under vacuum. The chemical composition and purity of **L** were confirmed by a combination of analytical and spectroscopic techniques. Elemental analysis is in agree with the molecular formula of **L**. IR spectrum show bands corresponding to the main functional groups of **L**, aromatic C – H in 3121, C = C in 1633 and C = N in 1514 cm^{-1}. The ESI-MS spectrum displayed a parent peak of high intensity at m/z 399.16, corresponding to **L**. NMR ^{1}H spectrum showed five signals that confirms the magnetic equivalence of protons due to the symmetry of the ligand.

Insert Figure 1

The platinum-tetrapyrazole complexes **1** and **2** were synthesized at room temperature by the reaction of $K_2[PtX_4]$ with **L** in a water/methanol mixture. In the case of **1**, **L** displaced two labile iodide ligands, while in **2**, **L** displaced two chloride ligands. Elemental analyses of these complexes are in agreement with the molecular formula proposed. The IR spectra of these platinum complexes displayed peaks clearly associated with the characteristic functional groups of the pyrazole derivative ligand. The bands in the range of the C=N and C=C absorption stretching vibration in the spectra of complexes **1** and **2** were shifted to 10 and 4 cm^{-1}

respectively, compared to those of the free **L**, attributable to binding of this to the metallic center [39]. The ESI-MS spectrum of complex **1** displayed parent peaks of high intensity with the platinum isotopic distribution corresponding to its molecular ion M-I at m/z 1168.84, while complex **2** showed a high intensity ion peak at m/z 895.09 corresponding to M-Cl. All NMR signals could be unequivocally assigned on the basis 1D and 2D, correlation spectroscopy (COSY) and heteronuclear multiple quantum correlation (HMQC). We have used the ^{1}H chemical shift variation of each signal with respect to those of the free ligand as a parameter to deduce the mode of binding of **L** to the metal. It has been previously shown that the largest variations are always observed for the protons located in the vicinity of the N-atom attached to the metal [40,41]. The spectra of all compounds are quite similar. Complexes showed a ^{1}H NMR spectrum in solution with five signals, this is indicative that the symmetry observed in **L** was retained in the complexes. In **1** and **2**, the pyrazole H3´ protons were slightly displaced downfield (~ 0.15 ppm) with respect to the free **L**. The other protons were shifted less than 0.04 ppm with respect to the free **L**. This is considered an indicative that **L** is coordinated to platinum through the pyrazole nitrogen atoms. Based on this data, we propose a structure for **1** and **2** of one molecule of **L** bind to two metal centers, corresponding to 16-electron Pt(II) complexes in the usual d^{8} square planar coordination geometry. Nevertheless, two coordination modes could be encountered for the ligand in these complexes, coordination mode A (1,2-N,N-4,5-N,N) or coordination mode B (1,5-N,N-2,4-N,N) as can be seen in Figure 2. Due to the lack of an X-ray structure, we performed theoretical calculations in order to determine the most stable conformations of the two coordination modes.

Insert Figure 2

Computational methods

Several conformers were considered for each coordination mode (A and B). The energetic differences between the two modes are 12 and 9 kcal/mol, when the halogens are Cl and I, respectively. The most stable conformations for both coordination modes are presented in Figure 3, coordination mode A for the complex with I and B for Cl. Geometries for the mode A with Cl and mode B with I are equivalent to the ones in this figure so we omit them. Coordination mode B induces high stress over the benzene ring of the ligand, which is evidenced by the slight deformation of the planarity of this ring. This was not observed for coordination mode A which is able to relax its structure in a more effective way. In all cases, and independently of the

halogen atom selected, the ligand prefers to coordinate to each metal center by the nitrogen atoms of the pyrazole rings with coordination mode A. The Pt-ligand distances for coordination mode A are 2.18 Å and 2.22 Å when the halogens are Cl and I, respectively. The equivalent distances for the coordination mode B are 2.24 Å and 2.28 Å for Cl and I, respectively. These theoretical results also support the fact that the coordination mode around the Pt atom is square-planar [42].

Insert Figure 3

In summary, each complex molecule is formed by two metal centers with oxidation state +2, one ligand molecule, and four halogen ions. These features suggest the presence of bimetallic complexes with two tetracoordinate metal centers that show a square planar coordination mode.

DNA interaction studies

One of the most important intracellular targets for antitumor platinum complexes is DNA [43,44]. The ability of complexes **1** and **2** to interact with DNA was examined using spectroscopic titration, thermal denaturation and viscosimetric methods. Electronic absorption spectra are commonly employed to study the binding of complexes to DNA. A non-intercalative binding of drugs to the DNA helix has been characterized classically through absorption spectral titrations, by following the changes in absorbance and shift in wavelength [45,46]. The absorption spectra of complexes with increasing concentrations of DNA showed similar behavior for both complexes. The absorption spectrum for complex **2** is shown for illustration (Fig. 4).

Insert Figure 4

Both complexes displayed hypochromicity and isosbestic points. The corresponding binding constants (K_b) for the complexes are summarized in Table 1. The values lie within the interval for which a compound is considered to be interacting with DNA. Such interactions have been described in terms of reversible binds of hydrogen bridging or an electrostatic component between the complexes and the nucleic acid polymer [47].

Insert Table 1

The melting temperature (T_m) was determined from the thermal denaturation curves of DNA (Fig. 5) obtained as described above. The observed DNA melting temperature in the absence of the complexes studied was 79.0 ºC, while the T_m of DNA in the presence of complexes **1** and **2** were 75.7 and 75.9 ºC, respectively. This decrease in T_m indicates that the interaction of DNA with both complexes leads a slight destabilization of the DNA double helix [48].

Insert Figure 5

The viscosity experiments reveal changes in the length of the DNA double helix. Viscosity measurements are considered to be a valid method to determine intercalation or non intercalation binding of complexes to DNA. When a metal complex intercalates between base pairs, the length of DNA increases which leads to an increase in viscosity. On the other hand, a partial and/or nonclassical intercalation of the compounds with the DNA helix reduces its effective length and concomitantly its viscosity. Results of these viscosity measurements are shown in Fig. 6. **L** and **1** showed only a small variation in the relative viscosity when the concentrations of the compounds were increased. Complex **2** showed a decrease in the relative viscosity of the DNA. The decrease in the viscosity of the solution is indicative of interactions in which the compound may be binding electrostatically or by hydrogen bonding to the outside of the double-stranded DNA molecule, creating a contraction in the polymer surface, which is reflected in the decrease in viscosity [49]. The results do indicate that the complexes do not intercalate between the DNA bases [50,51].

Insert Figure 6

Studying the DNA interaction results, we could suggest both compounds, but specially complex **2,** interact with DNA primarily through noncovalent interactions as electrostatic contacts or hydrogen bonding through the biopolymer grooves, causing conformational changes in the DNA structure [52]. These results endorse further testing as possible anticancer agents.

Comet assay

The comet assay, or single-cell gel electrophoresis (SCGE) has become one of the standard methods for assessing DNA damage [53]. A representative image obtained from results for complex **2** at 10 μM is showed in Figure 7, indicating medium type 2 damage to the DNA,

according to Collins [53]. In most of the slides studied a clearly positive result was observed, suggesting that complex **2** induces DNA damage in vivo in the target cell. A type 4 pattern was observed at 30 μM, indicating severe damage to the cellular DNA at this concentration. These results suggest that DNA is a prime target for these promising complexes.

Insert Figure 7

TrxR Inhibition Assay

It is well known that the thioredoxin reductase system (TrxR) is involved in various biochemical pathways, including tumor formation. Their inactivation causes reduction in growth of tumor cells.[54] Various gold complexes showed TrxR inhibition due to the formation of a covalent bond between the gold atom and the selenium center of the enzyme [55]. In this study, the inhibitory potential of complexes **1** and **2** was studied using the DTNB reduction assay, using TrxR isolated from rat liver. This assay makes use of the fact that TrxR reduces the disulfide bond of DTNB giving rise to the formation of 2-nitro-5-thiobenzoic acid (TNB), which can be detected photometrically [56].TrxR activities in the presence of the complexes are shown in Figure 8 as percentages relative to the control. These data were used to calculate the 50% inhibitory concentration (IC_{50}) for each complex. Good activities were observed (Complex **1**= 3.9 nM, complex **2** = 3.5 nM) compared with the classic inhibitor Auranofin [57]. The mechanism for TrxR inhibitory activity is attributed to binding of the platinum atom to the enzyme selenium center, which is critical to TrxR catalytic activity [58]. Lack of function of TrxR implies arrest of division and cellular growth. These results suggest that TrxR may be a target for these complexes *in vivo*.

Insert Figure 8

Growth inhibition and cytotoxicity

The compounds were tested on six tumor cell lines, representing tumors of different origins (prostate, breast, lung, cervix and colon), in addition to a murine breast tumor line, which it is regularly use for *in vivo* testing of anticancer drugs. We used the SRB assay, which has the advantage over the more common tetrazolium assays as it distinguishes between a cytostatic effect, (reduction in cell proliferation) and a cytotoxic effect (decrease in the number of viable

cells). Cisplatin and transplatin were included as control drugs. Table 2 shows that only complex **2** inhibited growth of the cell lines. There no was indication of cytotoxicity over the range of concentrations tested. Complex **1** was less active, inhibiting cell growth (GI_{50}/ TGI) at concentrations below 6 μM only on the prostate cell line (PC3). Ligand **L** did not show either cytostatic or cytotoxic activity. Complex **2** was generally similar to cisplatin in terms of its cytostatic activity against the cell lines, although it did not appear to be cytotoxic at the concentrations used in these experiments. It is interesting that the biological activity of complex **2** correlates with the stronger interaction observed with DNA and TrxR, compared to complex **1**.

Insert Table 2

Conclusion

Two platinum-pyrazole ligand complexes were synthesized and characterized by analytical and spectroscopic techniques. The spectroscopic and analytical results suggest a noncovalent interaction of the complexes with DNA, either electrostatic contacts and/or hydrogen bonding. The comet assay showed damage to cellular DNA. They both inhibited TrxR activity at very low concentrations, with **2** slightly more active than **1**. Both complexes exerted some degree of growth inhibition on the human tumor cell lines, higher than that shown by the free ligand, and both were more active than cisplatin against the prostate tumor cell line. As expected from the DNA and TrxR results, complex **2** showed greater activity against the tumor cells lines than complex **1,** and in the cases of two tumor cell lines, was more active than cisplatin. Complex **2** merits further study as a potential anticancer agent.

Acknowledgments

Authors are grateful to the personnel of the NMR, mass spectroscopy, IR and elemental analysis laboratories of the Chemistry Center at IVIC.

References

[1] Globocan 2012, IARC
[2] CP. Tan, YY. Lu, LN. Ji, ZW. Mao, Metallomics. 6 (2014) 978.
[3] B. Rosenberg, L. VanCamp, J.E. Trosko, V.H. Mansour, Nature. 222 (1969) 385.

[4] I. Ali, W.A. Wani, K. Saleem, A. Haque, Anticancer Agents Med. Chem. 13 (2013) 296.
[5] N.J. Wheatea, J.G. Collins, Curr. Med. Chem. - Anti-Cancer Agents. 5 (2005) 267.
[6] M.J. Hannon, Pure Appl. Chem. 79 (2007) 2273.
[7] E. Budzisz, M. Miernicka, I.P. Lorenz, P. Mayer, U. Krajewska, M. Rozalski, Polyhedron. 28 (2009) 637.
[8] V. Brabec, V. Kleinwâchter, J.L. Butour, N.P. Johnson, Biophys. Chem. 35 (1990) 129.
[9] M.A. Fuertes, J. Castilla, P.A. Nguewa, C. Alonso, J.M. Pérez, Medicinal Chemistry Reviews – Online. 1 (2004) 187.
[10] E. Budzisz, M. Miernicka, I.P. Lorenz, P. Mayer, U. Krajewska, M. Rozalski, Polyhedron. 28 (2009) 637.
[11] D.C.G.A. Pinto, A.M.S. Silva, J.A.S. Cavaleiro, C. Foces-Foces, A.L. Llamas-Saiz, N. Jagerovic, J. Elguero, Tetrahedron. 55 (1999) 10187.
[12] G.R. Bebernitz, G. Argentieri, B. Battle, C. Brennan, B. Balkan, B.F. Burkey, M. Eckhardt, J. Gao, P. Kapa, R.J. Strohschein, H.F. Schuster, M. Wilson, D.D. Xu, J. Med. Chem. 44 (2001) 2601.
[13] M.J. Vitolo, V.E. Marquez, I. Hurtado, J. Med. Chem. 21 (1978) 692.
[14] R. Hirschmann, P. Buchschacher, N.G. Steinberg, J.H. Fried, R. Ellis, G.J. Kent, M. Tishler, J. Am. Chem. Soc. 86 (1964) 1520.
[15] A.A. Bekhit, H.M.A. Ashour, A.A. Guemei, Arch Pharm. 338 (2005) 167.
[16] P. Rathelot, N. Azas, H. El-Kashef, F. Delmas, C. Di Giorgio, P. Timon-David, J. Maldonado, P. Vanelle, Eur. J. Med. Chem. 37 (2002) 671.
[17] Z.K. Sweeney, S.F. Harris, N. Arora, H. Javanbakht, Y. Li, J. Fretland, J.P. Davidson, J.R. Billedeau, S.K. Gleason, D. Hirschfeld, J.J. Kennedy-Smith, T. Mirzadegan, R. Roetz, M. Smith, S. Sperry, J.M. Suh, J. Wu, S. Tsing, A.G. Villasenor, A. Paul, G. Su, G. Heilek, J.Q. Hang, A.S. Zhou, J.A. Jernelius, F.J. Zhang, K. Klumpp, J. Med. Chem. 51 (2008) 7449.
[18] F.K. Keter, M.J. Nell, B. Omondi, I.A. Guzei, J. Darkwa, J. Chem. Res. 5 (2009) 322.
[19] P. Dilipkumar, S. Supriyo, S. Shefali, Int. J. Pharm. Pharm. Sci. 2 (2012) 98.
[20] F.K. Keter, J. Darkwa, Biometals. 25 (2012) 9.
[21] A. Budakoti, M. Abid, A. Azam, Eur J. Med. Chem. 42 (2007) 544.
[22] M. Navarro, W. Castro, A.R. Higuera-Padilla, A. Sierraalta, M.J. Abad, P. Taylor, R.A. Sánchez-Delgado, J. Inorg. Biochem. 105 (2011) 1684.
[23] C.M. Hartshorn, P.J. Steel, Aust. J. Chem. 48 (1995) 1587.
[24] A. Inc., DMol3 is available as part of Material Studio (2010).
[25] B. Delley, J. Chem. Phys. 92 (1990) 508.
[26] B. Delley, J. Chem. Phys. 113 (2000) 7756.
[27] J.P. Perdew, Y. Wang, Phys. Rev. B. 45 (1992) 13244.
[28] P.J. Hay, W.R. Wadt, J. Chem. Phys. 82 (1985) 299.
[29] J. Marmur, J. Mol. Biol. 3 (1961) 208.
[30] J.K. Barton, A. Danishefsky, J. Goldberg, J. Am. Chem. Soc. 106 (1984) 2172.
[31] X.W. Liu, J. Li, H. Li, K.C. Zheng, H. Chao, L.N. Ji, J. Inorg. Biochem. 99 (2005) 2372.
[32] M.E. Reichmann, S.A. Rice, C.A. Thomas, P. Doty, J. Am. Chem. Soc. 76 (1954) 3047.
[33] M. Navarro, C. Hernandez, I. Colmenares, P. Hernandez, E. Fernandez, A. Sierraalta, E. Marchan, J. Inorg. Biochem. 101 (2007) 111.
[34] A. Martínez, C.S.K. Rajapakse, B. Naoulou, Y. Kopkalli, L. Davenport, R.A. Sánchez-Delgado, J. Biol. Inorg. Chem. 13 (2008) 703.

[35] M. Navarro, A.R. Higuera-Padilla, M. Arsenak, P. Taylor, Transition Metal Chemistry. 34 (2009) 869.
[36] R.R. Tice, G.H. Strauss, Stem Cells. 1 (1995) 207.
[37] J. Fang, J. Lu, A. Holmgren, J. Biol. Chem. 280 (2005) 25284.
[38] P. Skehan, R. Storeng, D. Scudiero, A. Monks, J. McMahon, D. Vistica, J.T. Warren, H. Bokesch, S. Kenney, M.R. Boyd, J. Natl. Cancer Inst. 82 (1990) 1107.
[39] E. Budzisz, M. Miernicka, I.P. Lorenz, P. Mayer, U. Krajewska, M. Rozalski, Polyhedron. 28 (2009) 637.
[40] M. Navarro, E.J. Cisneros-Fajardo, T. Lehmann, R.A. Sánchez-Delgado, R. Atencio, P. Silva, R. Lira, J.A. Urbina, Inorg. Chem. 40 (2001) 6879
[41] M. Navarro, T. Lehmann, E.J. Cisneros-Fajardo, A. Fuentes, R.A. Sánchez-Delgado, P. Silva, J.A. Urbina, Polyhedron. 19 (2000) 2319
[42] T. Okada, I.M. El-Mehasseb, M. Kodaka, T. Tomohiro, K. Okamoto, H. Okuno, J. Med. Chem. 44 (2001) 4661.
[43] E. Wong, C.M. Giandomenico, Chem Rev. 99 (1999) 2451.
[44] E. R. Jamieson, S.J. Lippard, Chem. Rev. 99 (1999) 2467.
[45] L.M. Chen, J. Liu, J.C. Chen, C.P. Tan, S. Shi, K.C. Zheng, L.N. Ji, J. Inorg. Biochem. 102 (2008) 330.
[46] K. Abdi, H. Hadadzadeh, M. Weil, M. Salimi, Polyhedron. 31 (2012) 638.
[47] A. M. Pyle, J. P. Rehmann, R. Meshoyrer, C. V. Kumar, N. J. Turro, J. K. Barton, J. Am. Chem. Soc. 111 (1989) 3051.
[48] G. Lenglet, M.H. David-Cordonnier, Journal of Nucleic Acids. 2010 (2010) 290935.
[49] C. Robledo-Luiggi, W.D. Wilson, E. Pares, M. Vera, C.S. Martínez, D. Santiago, Biopolymers. 31 (1991) 907.
[50] S. Satyanarayana, J.C. Dabrowiak, J.B. Chaires, Biochemistry. 31 (1992) 9319.
[51] M. Navarro, A. Betancourt, C. Hernández, E. Marchán, J. Braz. Chem. Soc. 19 (2008) 1355.
[52] S. Kashanian, N. Shahabadi, H. Roshanfekr, K. Shalmashi, K. Omidfar, Biochemistry (Moscow). 73 (2008) 929.
[53] A.R. Collins. Molecular Biotechnology. 26 (2004) 249.
[54] S.J. Berners-Price, A. Filipovska, Metallomics. 3 (2011) 863.
[55] S. Nobili, E. Mini, I. Landini, C. Gabbiani, A. Casini, L. Messori, Med. Res. Rev. 30 (2010) 550.
[56] A. Holmgren, M.Bjornstedt, Meth. Enzymol. 252 (1995) 199.
[57] L. Messori, F. Abbate, G. Marcon, P. Orioli, M. Fontani, E. Mini, T. Mazzei, S. Carottie, T. O'Connell, P. Zanello, J. Med. Chem. 43 (2000) 3541.
[58] E.S.J. Arnér, H. Nakamura,T. Sasada, J. Yodoi, A. Holmgren, G. Spyrou, Free Radical Biology & Medicine. 31 (2001) 1170.

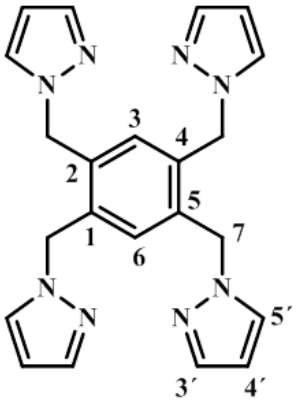

Figure 1. Structure of **L**.

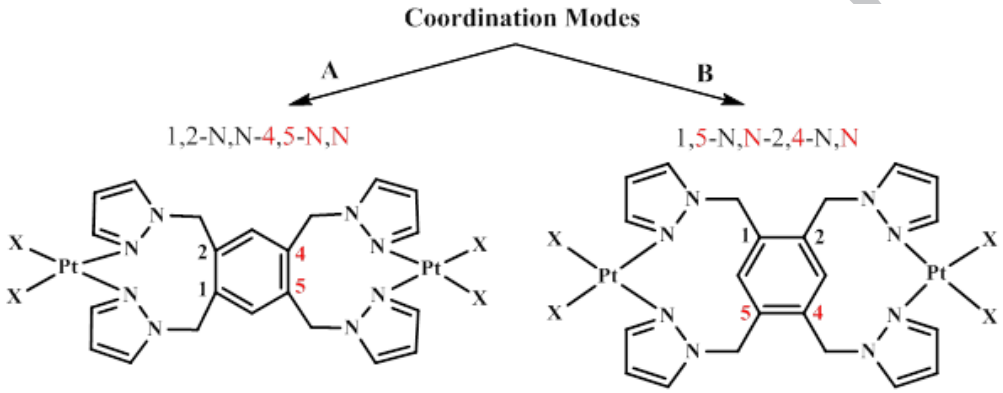

Figure 2. Possible coordination modes for the ligand in the studied compounds.

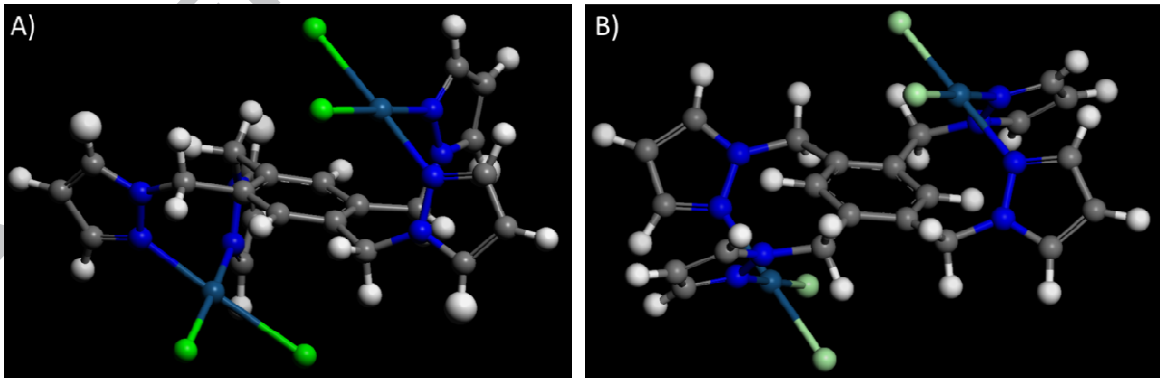

Figure 3. Most stable conformations for both coordination modes. A) Coordination mode A for the complex when the halogen is I. B) Coordination mode B for the complex when the halogen is Cl.

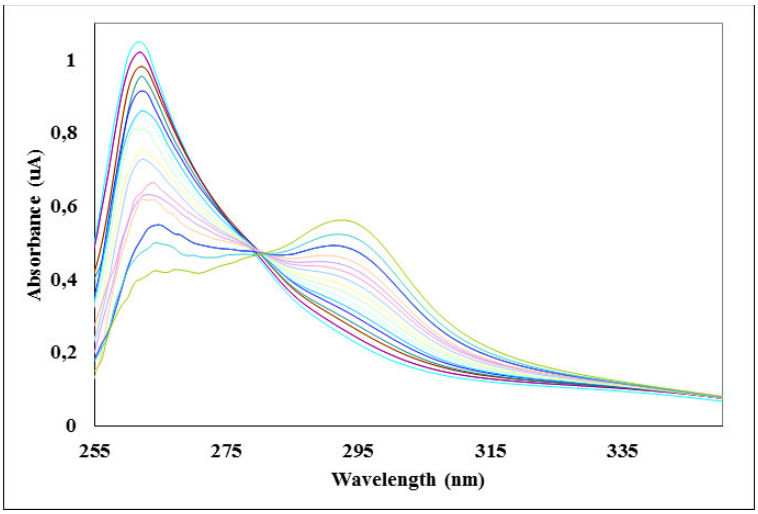

Figure 4. Spectroscopic titrations: [Complex 2] = $2 \cdot 10^{-4}$ M and [DNA] = 0.87 mg mL^{-1}.

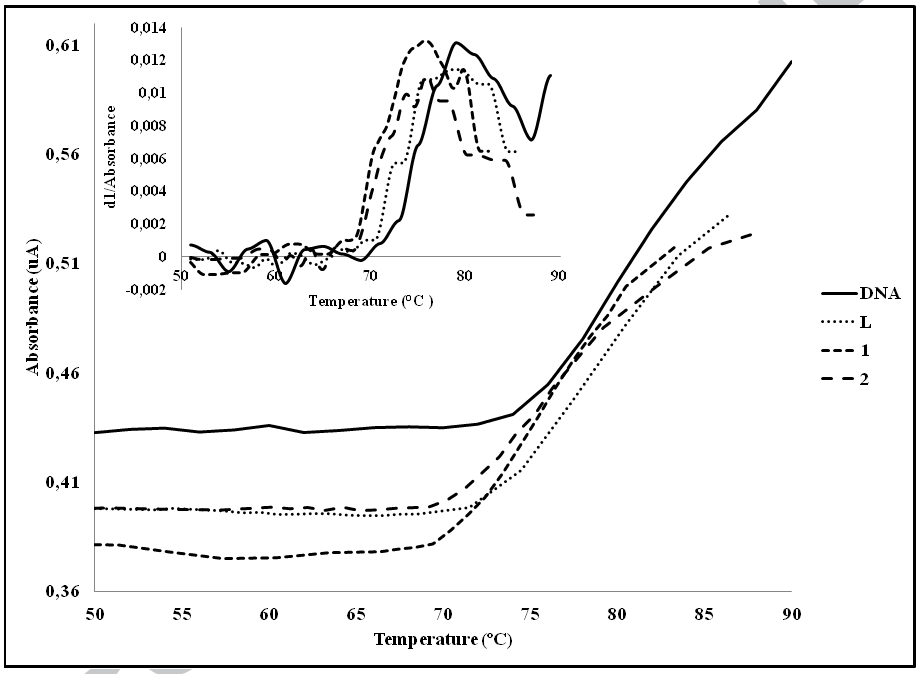

Figure 5. Thermal denaturation of DNA with the complexes with Ri = 0.2

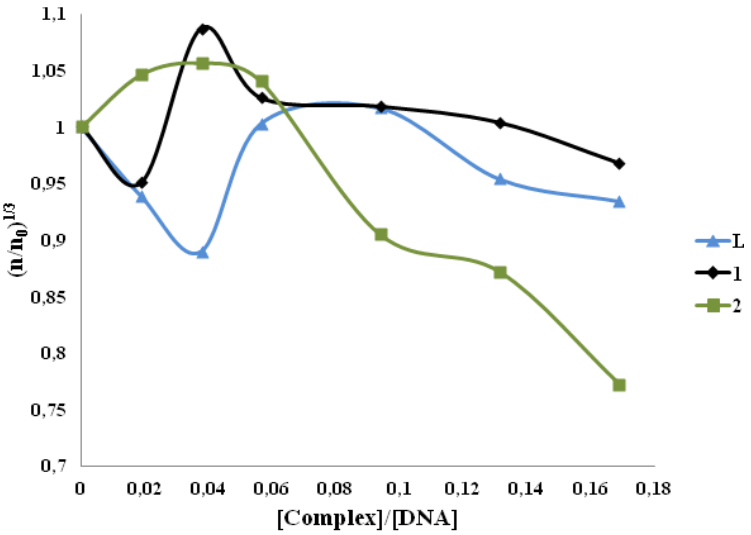

Figure 6. Effect of increasing concentration of the complexes on the relative viscosity of DNA at 25 ºC

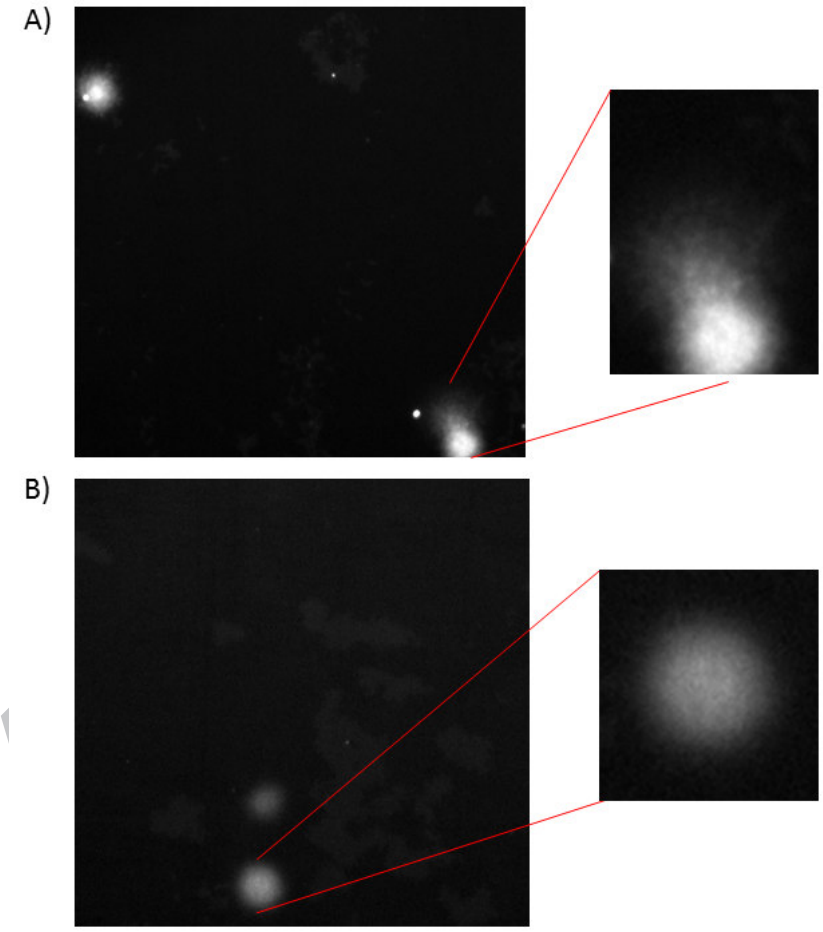

Figure 7. Cell DNA migration pattern for complex **2** produced by the single cell gel/comet assay 20x A) 10 µM, B) 30 µM.

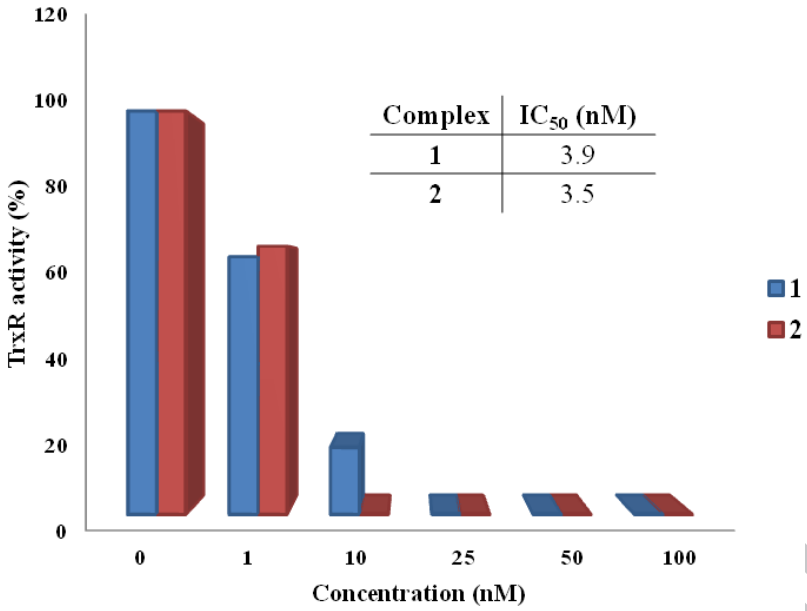

Figure 8. Thioredoxin reductase activity at different concentration of the complexes.

Table 1 Data obtained from different spectroscopic and analytical methods for DNA interaction with complexes **1** and **2**

Property	**1**	**2**
Absorbance (nm)	262	264
K_b (10^3 M^{-1})	1.10	2.25
Hypochromism (%)	89	69
Isosbestic point (nm)	302	279
Melting temperature (ºC)	75.7	75.9

Table 2 Cytostatic and cytotoxic effects of the platinum compounds against six tumor cell lines

	MCF7			**PC3**			**A549**			**HeLa**			**HT29**			**4T1**		
Compound	**GI_{50}**	**TGI**	**LC_{50}**	**GI_{50}**	**TGI**	**LC_{50}**	**GI_{50}**	**TGI**	**LC_{50}**	**GI_{50}**	**TGI**	**LC_{50}**	**GI_{50}**	**TGI**	**LC_{50}**	**GI_{50}**	**TGI**	**LC_{50}**
L	>30	>30	>30	>30	>30	>30	>30	>30	>30	>30	>30	>30	>30	>30	>30	>30	>30	>30
1	>30	>30	>30	**0,1**	**5,4**	>30	>30	>30	>30	>30	>30	>30	>30	>30	>30	>30	>30	>30
2	**8,7**	>30	>30	**0,1**	**14,7**	>30	**4,9**	**7,5**	>30	**2,4**	29	>30	**1,6**	**9,7**	>30	**4,6**	**9,3**	>30
Cisplatin	**0,2**	>30	>30	**0,7**	**20,9**	>30	**2,4**	**6,5**	**20,5**	**2,4**	**7,6**	**20**	**3,8**	**8,7**	**19,2**	**2**	**6,3**	**9,8**
Transplatin	>30	>30	>30	0,20	>30	>30	>30	>30	>30	>30	>30	>30	>30	>30	>30	>30	>30	>30

Cell viability was measured by the Sulphorhodamine B chromogenic assay after 48 h incubation in the presence of the complexes (μM). GI_{50} - 50% growth inhibition, TGI - total growth inhibition, LC_{50} - 50% cytotoxicity.

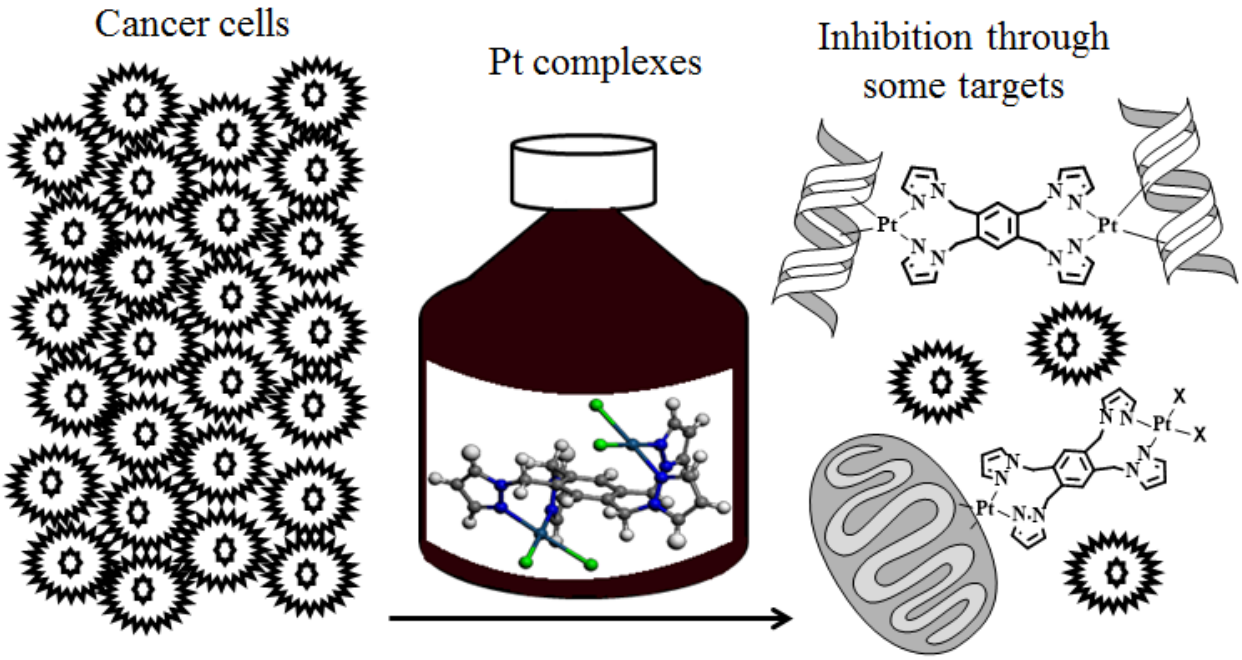

Synthesis, characterization and biological activity of two new platinum complexes is described. One of those complexes showed inhibitory effects on six tumor cell lines. The activity was attributed to inhibition of two targets, DNA and thioredoxin reductase.